Stability Analysis and Resonance Damping of LC Filter-Based Voltage Source Converter With Single-Loop Voltage Control

Aravind G, Divyanshu Bansal, L Umanand
Department of Electronics Systems Engineering
Indian Institute of Science
Bengaluru, India
aravindg@iisc.ac.in, divyanshub@iisc.ac.in, lums@iisc.ac.in

***Abstract*—This paper presents a lead compensator-based voltage control and resonance damping of a single-loop LC filter-based Voltage Source Inverter (VSI). Passive damping approaches lead to additional losses in the system; hence active methods to damp the filter resonances are widely utilized. Active methods either need additional current sensors or current estimator. In this paper, the effect of an undamped LC resonance on the system transfer functions is discussed and a lead compensator-based control system is designed to improve the system stability, thereby consequently damping the resonance in the output impedance transfer function as well. A detailed mathematical analysis is provided along with simulation and experimental results to validate the concept.**

***Index Terms*—Filter resonance, Active damping (AD), stability, output impedance, Voltage Source Inverter (VSI).**

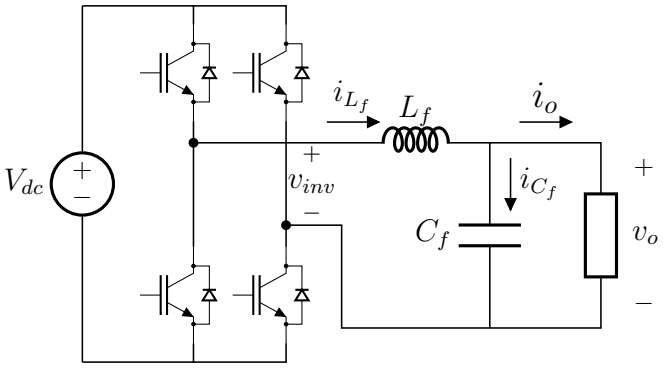

Fig. 1. LC filter-based 1-ϕ VSI with load.

I. Introduction

Voltage Source Inverter (VSI) systems with LC filter-based voltage control are widely used in applications where output voltage quality is crucial, such as Uninterruptible Power Supplies (UPS), Dynamic Voltage Restores (DVR), grid emulators, Grid Forming Inverters (GFM) [1] [2]. The second-order filtering provides more attenuation to the harmonic voltages present due to the inverter switching as well as a better output impedance profile, thus providing much better output quality when compared to a first-order filter. However, the issue of resonance in the second-order filter must be properly addressed in order to have stable operation of the control system. Passive damping of filter resonance leads to additional power loss in the system and hence damping techniques that combine resistors with capacitors or inductors (and their variants) have been explored to reduce the power dissipation [3]. Active damping methods involves the synthesis of virtual resistors [4] to achieve a virtual damping effect. Like in the passive case, synthesis of combinations of the vitual elements have also been analyzed [5]. However, they typically require additional current sensors in the case of inductor or load current sensing which increases the system cost, or a current estimator for capacitor current-based active damping.

For the output voltage control, both single and multi-loop voltage control methods are discussed in literature. Multi-loop control involves the typical inner current and outer voltage control loops [6]. The outer voltage control loop provides the reference for the inner current loop in which either the filter inductor or filter capacitor current is controlled. Since tight current control is typically not required, a proportional controller-based control is often utilized in practice. A rearrangement of the proportional gain of the current loop into the feedback and reference path reveals that it actually emulates either an inductor or capacitor current-based AD, depending on which current is being sensed [7].

In this paper, a single-loop control structure is realized using a Proportional-Resonant (PR) controller in cascade with a lead compensator. PR controller helps achieve zero steady-state error at its resonant frequency, which will be the required fundamental frequency, while the lead compensator provides the necessary phase gain at the gain crossover frequency (ω_{gc}) of the open-loop gain transfer function, thus improving the phase margin and relative stablity of the system. The phase improvement consequently provides sufficient damping required in the output impedance transfer function at and around the filter resonant frequency. Simulation and experimental results presented shows the effectiveness of the lead compensator in damping the filter resonance. The rest of the paper organization is as follows. Section II gives a brief system description along with the mathematical model. The issues associated with the open-loop operation is discussed. Section III describes the

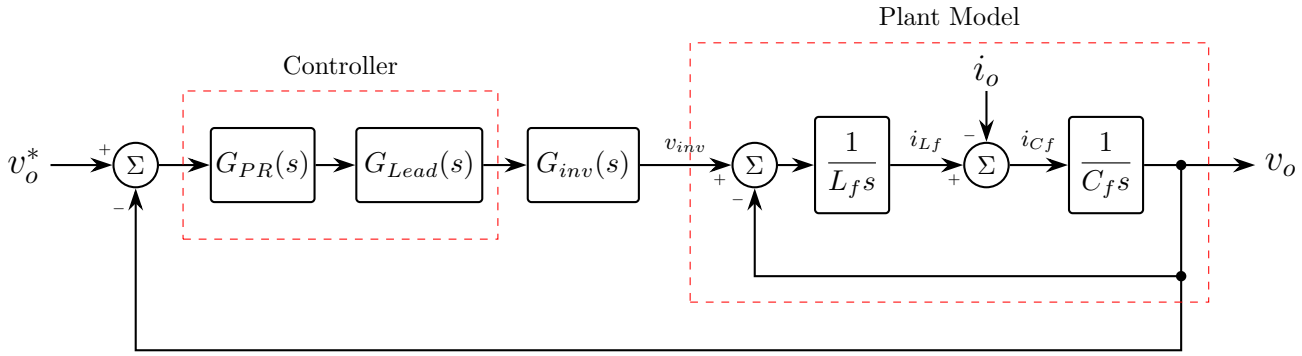

Fig. 2. Lead compensator-based single-loop voltage control block diagram.

controller structure along with the relevant frequency domain plots. The simulation and experimental results are discussed in section IV. Section V concludes the document.

II. System Description

The circuit schematic of the system is shown in Fig. 1. It consists of a 1-ϕ VSI cascaded with a second order LC filter. Refering to Fig. 1, the expression for the output voltage (v_o) in Laplace domain can be written as:

$$v_o(s) = \frac{1}{s^2/\omega_f^2 + 1} v_{inv}(s) - \frac{L_f s}{s^2/\omega_f^2 + 1} i_o(s)$$

$$= G_p(s) \times v_o^*(s) + Z_{out_{OL}}(s) \times [-i_o(s)] \quad (1)$$

where,

$G_p(s)$ - Plant transfer function

$Z_{out_{OL}}$ - Open-loop output impedance transfer function

It can be observed from the above equation that the undamped filter resonance causes resonant poles to appear in both the transfer functions. The sharp transition of the phase of the plant from 0° to -180° at the resonant frequency degrades the phase margin of the overall control system, thus leading to an oscillatory behaviour during closed-loop operation theoretically, but can lead to instability because of the delays present in a practical system. On the other hand, the infinite resonant gain in $Z_{out}(s)$ can cause even the smallest disturbance input (persistent or otherwise) to get amplified. Thus, the above problems need to be addressed for the stable operation of the closed-loop control system. Hence, the controller needs to improve the phase in the open-loop transfer function (loop gain) and damp the resonance in the output impedance.

III. Controller Structure and Closed-loop Transfer Functions

The block diagram of the closed-loop control system is depicted in Fig. 2. The controller part, as indicated in Fig. 2 uses a Proportional-Resonant (PR) controller cascaded with a lead compensator.

A. PR Controller

The PR controller can be tuned to provide a very large gain at the resonant frequency (50 Hz), thereby resulting in zero steady-state error for a 50 Hz reference input. The transfer function of the PR controller is given as

$$G_{PR}(s) = K_{pr} + \frac{K_{ir} s}{s^2 + \omega_r^2}$$

$$= K_{pr} \frac{s^2 + \frac{K_{ir}}{K_{pr}} s + \omega_r^2}{s^2 + \omega_r^2} \quad (2)$$

The controller gain K_{pr} affects the overall gain while the ratio of $\frac{K_{ir}}{K_{pr}}$ affect the damping of the zero and hence widens the gain around the resonant frequency and also increases the frequency range upto which the phase lag of the PR controller persists. Here, the PR controller gains are chosen in such a way that a desired minimum gain is obtained in a ± 2 Hz band around the resonant frequency of 50 Hz. This limits the influence of the phase of the PR block to a limited region, which is desirable since that phase lag is not desired at and around the unity gain crossover frequency of the loop gain.

B. Lead compensator

The lead compensator is cascaded with the PR controller in order to provide additional phase lead at and around the gain crossover frequency of the loop gain . The transfer function of the lead compensator is given as

$$G_{Lead}(s) = G_o \frac{1 + s/\omega_z}{1 + s/\omega_p}, \quad \omega_p > \omega_z$$

The maximum phase lead for a lead compensator occurs at the geometric mean of the pole and zero frequencies and hence the by selecting the gain crossover frequency as the geometric mean, maximum phase lead can be achieved. However, this method requires the gain (G_o) of the compensator to be less than one since the placement of the zero and pole to the left and right respectively, of the required crossover frequency causes it to shift to the right. Since further reduction in gain is not desired in this system, the zero of the lead compensator is placed exaclty at the filter pole location, which helps to achieve a phase margin of about 50° at ω_{gc} (which is typically chosen

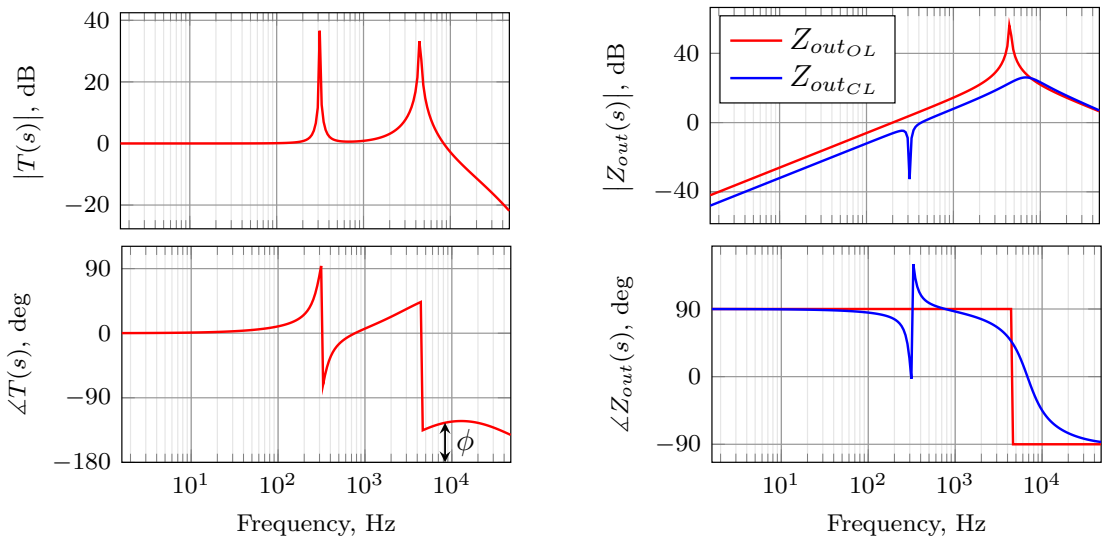

Fig. 3. Frequency response plots of (a) Compensated Loop gain, $L(s)$, (b) Output impedance, $Z_{out}(s)$

very close to the filter resonant frequency). Also, considering a $\pm 15\%$ varation in the pole location to the change in the filter parameters, a reasonable phase margin can still be achieved without too much deviation in ω_{gc}.

C. Power amplifier block

The power amplifier, which is the VSI, can be modelled as a gain with a delay period of one sampling interval (T_s). Double sampling, where the computation and PWM updation is done twice in a carrier cycle, is utilized. Thus, $G_{inv}(s) = V_{dc}e^{-sT_s}$. This block adds an additional phase lag of 36° and and 18° at $\left(\frac{1}{10}\right)^{th}$ and $\left(\frac{1}{20}\right)^{th}$ of the sampling frequency (F_s) respectively. This additional phase lag is taken into consideration for checking the final available phase margin for the loop gain.

D. Closed-loop system

The expression for the output voltage of the closed-loop system as derived from the system block diagram in Fig. 2, is given as:

$$v_o(s) = \frac{L(s)}{1+L(s)}v_o^*(s) + \frac{Z_{out_{OL}}(s)}{1+L(s)}\left[-i_o(s)\right]$$

$$= T(s) \times v_o^*(s) + Z_{out_{CL}}(s) \times \left[-i_o(s)\right] \quad (3)$$

where,

$L(s)$ = $G_{PR} \times G_{Lead} \times G_{inv} \times G_P$, is the system loop gain (open-loop transfer function)

$T(s)$ - Transmission function (Reference-to-output transfer function)

$Z_{out_{CL}}$ - Closed-loop output impedance transfer function

TABLE I
SYSTEM PARAMETERS

Parameters	*Values*
Filter inductor, L_f	5mH
Filter capacitor, C_f	10 μF
Filter resonant frequency, ω_f	711 Hz
Switching frequency, F_{sw}	10 kHz
Sampling time, Ts	20 kHz

The frequency response plots for the loop gain ($L(s)$) along with the uncompensated and compensated output impedance transfer fucntions for the design parameters of Table. I is shown in Fig. 3. The magnitude plot in Fig. 3a exhibits high gain at both resonant integrator frequency (ω_o) and the filter resonant frequency (ω_f). It seems like the resonance is undamped even in the compensated open-loop gain. However, it is evident from the phase plot that due to the addition of the lead compensator, the sharp transition in the phase at the filter resonant frequency does not lead to instability. Also, sufficient phase margin is achieved.

Also, it can be observed from 3b that the resonant peak in the output impedance is effectively suppressed after the addition of the lead compensator. The high gain at the resonant frequency of the numerator and denominator polynomial of $Z_{o_{CL}}(s)$ gets subtracted, thereby limiting the gain to the value of the inductive reactance at the filter resonant frequency and producing a resistor-like effect in the gain plot at ω_f.

In addition, proper choice of the value of the filter components (for the same ω_f) can help bring down the gain further. The regulation performance of the system under harmonic disturbances can be addressed by using multi-resonant PR controllers [8] [9]. This however, not being the focus of this paper will, not be discussed.

IV. Results and Discussion

The system parameters used for simulation are shown in Table. I. The resonant frequency of the LC filter is selected close to $\left(\frac{1}{10}\right)^{th}$ of the switching frequency of the inverter. The simulation is performed using the switching model of the inverter with all the filter components being ideal. The simulation results for no-load condition is shown in Fig. 4a. The damping provided by external elements during the no-load condition is virtually zero. It can be seen that the lead compensator is stabilizing the system and the reference voltage is getting perfectly tracked. At a point in time (see Fig. 4a), the lead compensator is disables and then re-enabled again. It can be observed that due to the degradation of the relative stability of the system, the oscillations kick in immediately and starts to grow. After re-enabling the lead compensator, oscillations subside and the system stabilizes again in little more than one line cycle. Fig. 4b shows the simulation results for the steady state operation of the inverter when loaded with an inductive load of 2.5 kVA. It can be seen that the controller perfectly tracks the reference voltage, thus providing a good quality output voltage. Experimental results for no-load condition for a voltage reference peak of 150 V is shown in Fig. 5. The DC bus voltage is 200 V. It is evident that the lead compensator is able to stabilize the system and the reference voltage is getting perfectly tracked. Lead compensator is then disabled for 5 ms duration (shown by the bottom trace) and then re-enabled. It can be observed that oscillations at the filter resonant frequency is triggered immediately. However, because of the damping present in the practical system and also due to the reduced DC bus voltage, the peak voltage rise is not as high as in the simulation. The re-enabling of the compensator causes the oscillation to die down immediately. Experimental results thus show the effectiveness of the lead compensator in damping the system.

V. Conclusion

A single-loop voltage controlled LC filter-based VSI is presented. The issues caused by an undamped second order filter is discussed and a simple solution involving a lead compensator in cascade with a resonant controller is presented, which improves the phase margin of the system loop gain transfer function and consequently damps the resonant peak in the output impedance transfer function, thereby ensuring stable operation. Additional current sensor, which is typically used for active damping (in case of inductor and load current-based methods) can be done away with, thereby reducing the overall system cost. Simulation studies performed using the inverter switching model along with the experimental results validates the concept.

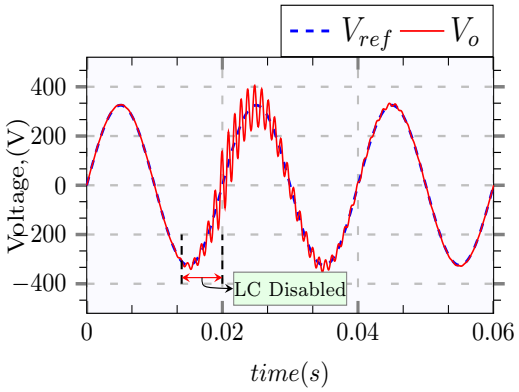

(a)

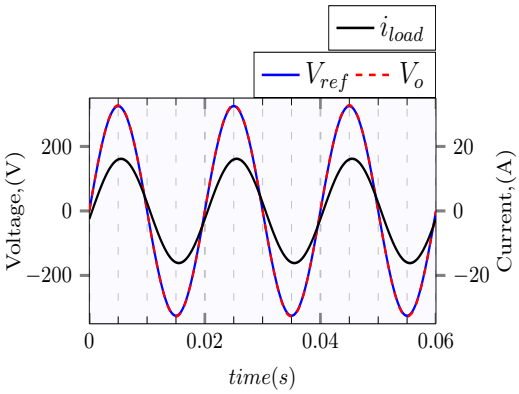

(b)

Fig. 4. Simulation results. (a) Lead compensator (LC) disabled for a short interval during no-load condition, (b) Steady-state performance for 2.5 kVA load

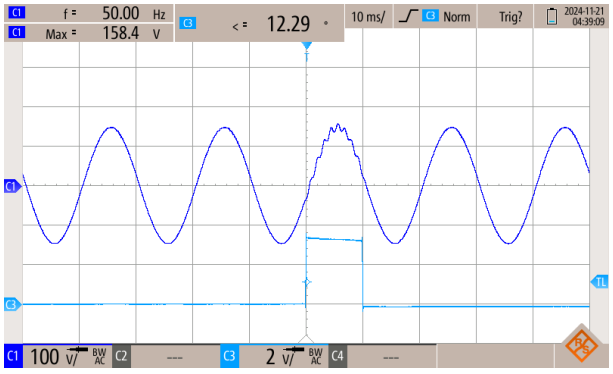

Fig. 5. Experimental results showing output voltage (C1), lead compensator disable and re-enable (C3) during no-load condition.

References

[1] Y. W. Li, "Control and resonance damping of voltage-source and current-source converters with lc filters," *IEEE Transactions on Industrial Electronics*, vol. 56, no. 5, pp. 1511–1521, 2009.

[2] X. Wang, Y. W. Li, F. Blaabjerg, and P. C. Loh, "Virtual-impedance-based control for voltage-source and current-source converters," *IEEE Transactions on Power Electronics*, vol. 30, no. 12, pp. 7019–7037, 2015.

[3] A. K. Balasubramanian and V. John, "Analysis and design of split-capacitor resistive-inductive passive damping for lcl filters in grid-connected inverters," *IET Power Electronics*, vol. 6, no. 9, pp.

1822–1832, 2013. [Online]. Available: https://ietresearch.onlinelibrary.wiley.com/doi/abs/10.1049/iet-pel.2012.0679

[4] P. Dahono, Y. Bahar, Y. Sato, and T. Kataoka, "Damping of transient oscillations on the output lc filter of pwm inverters by using a virtual resistor," in *4th IEEE International Conference on Power Electronics and Drive Systems. IEEE PEDS 2001 - Indonesia. Proceedings (Cat. No.01TH8594)*, vol. 1, 2001, pp. 403–407 vol.1.

[5] X. Wang, F. Blaabjerg, and P. C. Loh, "Virtual rc damping of lcl-filtered voltage source converters with extended selective harmonic compensation," *IEEE Transactions on Power Electronics*, vol. 30, no. 9, pp. 4726–4737, 2015.

[6] P. C. Loh, M. Newman, D. Zmood, and D. Holmes, "A comparative analysis of multiloop voltage regulation strategies for single and three-phase ups systems," *IEEE Transactions on Power Electronics*, vol. 18, no. 5, pp. 1176–1185, 2003.

[7] V. Blasko and V. Kaura, "A novel control to actively damp resonance in input lc filter of a three-phase voltage source converter," *IEEE Transactions on Industry Applications*, vol. 33, no. 2, pp. 542–550, 1997.

[8] L. F. A. Pereira, J. V. Flores, G. Bonan, D. F. Coutinho, and J. M. G. da Silva, "Multiple resonant controllers for uninterruptible power supplies—a systematic robust control design approach," *IEEE Transactions on Industrial Electronics*, vol. 61, no. 3, pp. 1528–1538, 2014.

[9] F. Hans, W. Schumacher, S.-F. Chou, and X. Wang, "Design of multifrequency proportional–resonant current controllers for voltage-source converters," *IEEE Transactions on Power Electronics*, vol. 35, no. 12, pp. 13 573–13 589, 2020.